Phospholipid Scramblase Activation Pathways in Lymphocytes†

Patrick Williamson,*,‡ Allison Christie,‡ Torvald Kohlin,‡ Robert A. Schlegel,§ Paul Comfurius,|| Marjan Harmsma,|| Robert F. A. Zwaal,|| and Edouard M. Bevers||

Department of Biology, Amherst College, Amherst, Massachusetts 01002, Department of Biochemistry and Molecular Biology, Penn State University, University Park, Pennsylvania 16802, and Department of Biochemistry, CARIM, University of Maastricht, Maastricht, The Netherlands

Received August 15, 2000; Revised Manuscript Received March 28, 2001

ABSTRACT: In erythrocytes and platelets, activation of a nonspecific lipid flipsite termed the scramblase allows rapid, bidirectional transbilayer movement of all types of phospholipids. When applied to lymphoid cells, scramblase assays reveal a similar activity, with scrambling rates intermediate between those seen in platelets and erythrocytes. Scrambling activity initiated in lymphoid cells by elevation of intracellular Ca^{2+} proceeds after a lag not noted in platelets or erythrocytes. The rates of transbilayer movement of phosphatidylserine and phosphatidylcholine analogues are similar whether the scramblase is activated by elevated internal Ca^{2+} or by apoptosis. Elevation of internal Ca^{2+} levels in apoptotic cells does not result in an additive increase in the rate of lipid movement. In lymphoid cells from a patient with Scott syndrome, scramblase cannot be activated by Ca^{2+}, but is induced normally during apoptosis. These findings suggest that Ca^{2+} and apoptosis operate through different pathways to activate the same scramblase.

In virtually all normal cells of vertebrate and invertebrate animals, the lipids in one leaflet of the plasma membrane bilayer differ from those in the other leaflet, with phosphatidylcholine (PC)[1] and sphingomyelin (Sph) concentrated in the outer leaflet, and phosphatidylserine (PS) and the majority of phosphatidylethanolamine (PE) found in the inner leaflet (*1*−*3*). Translocation of PS and PE from the outer to the inner leaflet of the plasma membrane is driven by the aminophospholipid translocase (*4*), a P-type ATPase (*5*). Disruption of this normal lipid distribution is an important element in blood platelet activation (*6*) and in apoptosis (*7*). Loss of lipid asymmetry with concomitant PS exposure at the surface of activated platelets promotes assembly and catalysis of active enzyme−substrate complexes of the coagulation cascade, in particular the tenase and prothrombinase complexes. The appearance of PS on the surface of these cells depends on lipid scramblase activity, which catalyzes the randomization of membrane phospholipids (*8*, *9*). The scramblase, which can be activated by elevation of internal Ca^{2+} concentration, has been characterized in most detail in platelets, where it has been shown to catalyze both inward and outward transbilayer lipid movement at rates which are virtually identical for PC, PE, PS, and Sph (*10*). A very similar activity is present at much lower levels in human erythrocytes (*8*, *11*), and a candidate scramblase protein has been isolated and cloned from human erythrocytes (*12*). Ca^{2+}-induced lipid scrambling is defective in cells from patients with Scott syndrome, a rare autosomal bleeding disorder originating from a reduced ability of activated platelets to expose procoagulant phospholipids on their surface (*11*, *13*, *14*).

Loss of asymmetry and exposure of PS on the cell surface is also a general feature of apoptosis (*3*), being necessary and sufficient for the generation of signals which provoke recognition and phagocytosis of the apoptotic cell (*7*, *15*−*18*). The mechanism by which PS becomes exposed on apoptotic lymphocytes seems to be similar to the homologous process in platelets—a coordinate inhibition of aminophospholipid translocase activity and activation of lipid scramblase (*19*−*21*). The scramblase of lymphocytes can also be activated by artificially elevating cytosolic Ca^{2+} (*17*). Neither this activity nor the scramblase in any nucleated cell has been characterized in any detail, and activation induced by apoptosis and by elevating Ca^{2+} have not been compared. Here, we have applied several assays of transbilayer lipid movements to characterize the Ca^{2+}-activated and apoptosis-activated scramblase in a variety of lymphocytes, as well as the impact of the Scott mutation on the behavior of the scramblase in apoptotic lymphocytes.

EXPERIMENTAL PROCEDURES

Reagents. Eagle's medium with glutamine, RPMI-glutamax I, Hank's buffer, and fetal calf serum were from GIBCO BRL (Gaithersburg, MD), Lymphoprep was from Nycomed Pharma AS. (Oslo). The Ca^{2+} ionophore ionomycin and bovine serum albumin (BSA) were from Sigma (St Louis, MO). 1-Oleoyl-2-[6-[(7-nitro-2,1,3-benzoxadiazol-4-yl)amino]caproyl]-*sn*-glycero-3-phosphocholine (NBD-PC) and the corresponding phosphatidylserine analogue (NBD-PS) were

* To whom correspondence should be addressed.

† Supported by an RUI grant from the National Science Foundation (MCB-9319104) and by a grant from The Netherlands Foundation for Chemical Research (CW) with financial aid from The Netherlands Organization for Scientific Research (NWO) to M.H.

‡ Amherst College.
§ Penn State University.
|| University of Maastricht.

[1] Abbreviations: PS, phosphatidylserine; Sph, sphingomyelin; PE, phosphatidylethanolamine; PC, phosphatidylcholine; NBD, 6-[(7-nitro-2,1,3-benzoxadiazol-4-yl)amino]; EBV, Epstein−Barr virus; FS, forward scatter; SS, side scatter; PI, propidium iodide; BSA, bovine serum albumin; FITC, fluorescein isothiocyanate.

10.1021/bi001929z CCC: $20.00
Published on Web 06/12/2001

obtained from Avanti Polar Lipids (Alabaster, AL). FITC-labeled annexin V was a kind gift of Dr. C. P. M. Reutelingsperger. Calcium Green-5N (acetoxymethyl ester) was obtained from Molecular Probes (Eugene, OR).

Cell Culture. DO11.10 cells, a murine T cell hybridoma (a gift of Dr. B. Osborne, University of Massachusetts), were grown in Eagle's medium with glutamine, supplemented with 10% fetal calf serum. Jurkat cells were cultured in RPMI-glutamax I, supplemented with 10% fetal calf serum. Both cell lines were cultured at 37 °C in a 5% CO_2 humidified atmosphere and were transferred to fresh medium every 2 days. Where indicated, increased levels of apoptosis were induced by UV irradiation; cells in a standard 25 cm^2 tissue culture flask were placed on a Vilber Lourmat UV illuminator and exposed at 312 nm for 5 min.

EBV-Transformation of B Cells. Peripheral blood mononuclear cells were isolated from blood obtained from a patient with Scott syndrome and from a normal control using Lymphoprep. Briefly, anticoagulated whole blood was centrifuged and 1 vol of isolated buffy coat was layered on top of 0.7 vol Lymphoprep. After centrifugation at 400*g* for 20 min, the mononuclear cell fraction was washed twice with PBS containing 10% fetal calf serum and resuspended at 5×10^6/mL in an EBV-containing supernatant kindly provided by Dr. S. H. van der Burg (Academic Hospital, Leiden, Netherlands) followed by incubation for 1 h at 37 °C under gentle shaking conditions. Cells were washed and resuspended in RPMI-glutamax I supplemented with 10% fetal calf serum and 1 mg/mL cyclosporin A (Sandoz) to a final concentration of 10^6 cells/ml. Cells were seeded in a 96-well plate (100 μL/well). When proliferating B cells appeared, they were combined and transferred to 48-well plates and finally to culture flasks, containing RPMI-glutamax I containing 10% fetal calf serum; cyclosporin was no longer present at this stage. Cells were kept at 37 °C in a humidified atmosphere with 5% CO_2 and were diluted in 3 vol fresh medium every 2 or 3 days.

Continuous Assay for Measuring Lipid Analogue Translocation by Spectrofluorimetry. A continuous fluorimetric assay, described previously for platelets (*22*), was used to monitor the outward movement of NBD-PS from DO11.10 cells. Cells at a concentration of 10^7/ml were allowed to internalize NBD-PS (1.7 mM) for 10 min at 20 °C and then were resuspended at 10^6 cells/mL in 3 mL Hank's buffer containing 1 mM $MgCl_2$ and 0.1 mM EGTA. The fluorescence signal of the labeled cells was continuously monitored in an LS50-B Perkin-Elmer spectrofluorimeter using excitation at 465 nm and emission at 535 nm. Sodium dithionite (from a freshly prepared 1.0 M stock solution in 1.0 M Tris base) was added to the stirred cuvette to a final concentration of 20 mM; this reducing agent chemically abolishes the fluorescence signal of the probe in the outer leaflet of the membrane (*23*). $CaCl_2$ in various concentrations up to 1 mM and ionomycin at 6 μM were added; these could be added in either order, but addition of both was required to initiate the lipid scrambling process. Blank values were obtained by addition of Triton X-100 to a final concentration of 0.3% to make all probe accessible to dithionite. Two methods were used for determining the lag before the onset of scrambling. At low Ca^{2+} concentrations, the length of the lag was determined by calculating the second derivative from the continuous fluorescence recording (like that shown in Figure 1). The maximum in the second derivative curve, representing the inflection point in the fluorescence decay curve, was taken as the onset of lipid scrambling. At higher Ca^{2+} concentrations, the lag time was more conveniently determined by curve fitting the fluorescence data before and after addition of Ca^{2+}. The point where extrapolations of these fits cross was designated as the end of the lag period. Where both methods could be applied, they gave similar results for the boundary between the lag phase and the onset of scrambling.

Continuous Assay for Monitoring Loss of Lipid Asymmetry by Flow Cytometry. FITC-labeled annexin V was used to detect the appearance of PS at the cell surface. Briefly, 10 μL of cell suspension (approximately 10^7/mL) was diluted in 500 μL Hepes buffer (10 mM Hepes and 150 mM NaCl, pH 7.4), containing 2.5 mM $CaCl_2$, 0.5 mg/mL FITC-labeled annexin V, and 20 mg/mL propidium iodide (PI) to check for membrane integrity. Scrambling was initiated by the addition of ionomycin to a final concentration of 4 μM from a 5 mM stock in ethanol. A23187 (Calbiochem) was occasionally substituted for ionomycin, with similar results. The incubation tube was then sampled continuously in a flow cytometer (Coulter Epics XL-MCL), and forward scatter (FS), side scatter (SS), annexin V (log green fluorescence), and PI (log red fluorescence) data were continuously analyzed for 600−1000 s. The collected data were analyzed using WinMDI software (http://facs.scripps.edu) and time versus fluorescence data from gated populations exported into SigmaPlot (Jandel Scientific), where fluorescence averages were calculated for all the cells in each time bin; the resulting averages were normalized to the average intensity of the apoptotic cells in the same population, and the result was plotted versus time.

A similar protocol allowed substitution of FM1−43 for annexin to measure loss of lipid asymmetry (*24*). FM1−43 (Molecular Probes, Eugene, OR) was added to a final concentration of 3 μM from a stock solution in DMSO. The concentration of the stock was determined from the absorbance at 510 nm, assuming a molar extinction coefficient of 5.6×10^4. Fluorescence was measured in the green channel (FL1). The broad emission spectrum of FM1−43 precluded the simultaneous use of other probes, including PI, so that only cells in the viable (FS/SS) fraction (which are all PI negative) could be analyzed by this method.

Uptake of NBD-Lipid Analogues Measured by Flow Cytometry. Cell suspensions were centrifuged as above and the cell pellet was resuspended in RPMI without fetal calf serum to remove albumin from the medium; 125 μL of cell suspension (10^7 cells/ml) was diluted in 125 μL of Hepes buffer containing 1 mM $CaCl_2$, pH 7.4, and PI was added to 20 μg/mL. NBD-PS or NBD-PC, dried from a 1 mM stock in $CHCl_3$ under a flow of nitrogen, was resuspended at a concentration of 0.1 mM in Hepes buffer and 1 μL of this suspension was added to the cells to initiate uptake. In some experiments, lipid scrambling was induced by addition of 0.25 μL of ionomycin (5 mM in DMSO) 5 min prior to addition of NBD-lipid analogues. Following addition of probe, 25 μL samples were taken at indicated time intervals and diluted into 0.375 mL of precooled (0 °C) Hepes buffer containing 1% fatty acid free BSA to extract label remaining in the outer leaflet of the membrane. For measuring total fluorescence, samples were mixed with Hepes buffer in

absence of BSA. After 2 min extraction time, samples were introduced into the flow cytometer, and listmode data collected for 10 000 cells, measuring forward scatter, side scatter, log green fluorescence (NBD signal), and PI fluorescence. The listmode data were subsequently analyzed using the WinMDI 2.7 software program. PI-positive cells were removed from the analyzed population, and two-dimensional FS/SS plots were used to distinguish morphologically normal from morphologically apoptotic (lower FS, higher SS) populations (see Figure 7). Unless otherwise indicated, ionophore-induced movements were measured only on the morphologically normal cell population (selected by gating). Lipid movements in apoptotic cells were generally measured in spontaneously apoptotic cells in EBV-transformed B cell populations; these cells were identified and gated from FS/SS plots as illustrated in Figure 9. Fraction of probe incorporated was determined by dividing the median NBD fluorescence of the sample population after BSA extraction (internalized probe) by the median NBD fluorescence of the same population in the absence of BSA (total bound probe). The amount of total bound probe was a function of the amount of NBD-lipid added, since virtually all of the added label was taken up by the cells.

Ca^{2+} Uptake Assay. DO11.10 cells, at a concentration of 10^6/mL in Hank's buffer containing 1 mM $MgCl_2$ and 0.1 mM EGTA, were loaded with 8 mM Calcium Green-5N (Molecular Probes) for 10 min at 20 °C. After washing, cells were resuspended in Hank's buffer to a concentration of 10^7/mL. The probe signal was measured continuously at 535 nm (excitation at 488 nm) during which ionomycin and variable concentrations of Ca^{2+} were added.

RESULTS

The most detailed analyses of scramblase function have come from an assay measuring transbilayer movement of NBD-labeled phospholipid analogues. Cells are first allowed to internalize the analogue, then cellular fluorescence is measured continuously in medium containing the impermeant reducing agent sodium dithionite, which reduces the NBD group to a nonfluorescent amine derivative (*23*). Activation of scramblase results in externalization of the internalized probe and a decrease in cellular fluorescence as the probe reaches the cell surface and is reduced. Using this assay with a murine T-lymphoma cell line, DO11.10, activation of the scrambling process by ionophore and Ca^{2+} could be observed, as shown in Figure 1. The increased rate of NBD-PS externalization required elevation of internal Ca^{2+}, since neither ionophore alone, nor Ca^{2+}alone (data not shown), produced this effect. Neither this increased rate nor the background rate seen in the absence of Ca^{2+} or ionophore was due to dithionite penetration into the cell interior, since neither showed a dependence on the concentration of added dithionite (data not shown). As shown in Figure 2, scramblase is activated at external Ca^{2+} levels of 25 μM or higher, and reaches maximal levels at about 100 μM, compared to platelets and erythrocytes where scramblase activation occurs at external Ca^{2+} levels of 50 μM or higher (*8*, *22*). There is some suggestion that scramblase activation is blunted at higher Ca^{2+} levels, a result previously observed in platelets (*22*) as well as erythrocytes (unpublished observation).

In contrast to nonnucleated cells, the onset of elevated NBD-PS movement in DO11.10 cells activated by Ca^{2+}

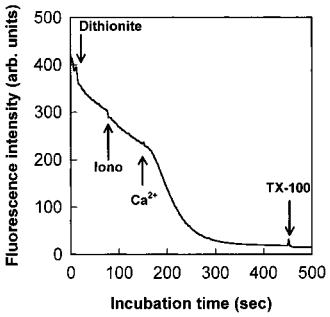

FIGURE 1: Activation of scramblase in DO11.10 cells by ionophore and Ca^{2+}, measured as the decay of the fluorescence of NBD-PS in the presence of dithionite. DO11.10 cells were loaded with NBD-PS for 10 min at 20 °C and diluted to a concentration of 10^6 mL^{-1} in 3 mL Hank's buffer containing 1 mM $MgCl_2$ and 0.1 mM EGTA. Dithionite (20 mM), ionomycin (6 μM), and Ca^{2+} (1 mM) were added as indicated by the arrows. Triton X-100 (0.3% final concentration) was added to make all NBD probe available to dithionite, thus allowing determination of the background fluorescence.

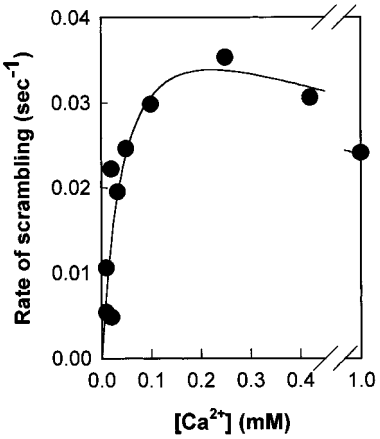

FIGURE 2: Rate of scrambling in DO11.10 cells as a function of the extracellular Ca^{2+} concentration. Conditions were as described for Figure 1, except for the concentration of Ca^{2+}, which was varied. For each condition, the first-order rate constant for fluorescence decay was determined for the portion of the activation curve following the lag, and this value was plotted versus the concentration of Ca^{2+} used. The value for the Ca^{2+} concentration is for the Ca^{2+} in excess of the EGTA in the solution, and is not adjusted for dissociation of Ca^{2+}/EGTA complexes. The rate of probe reduction in the absence of scramblase activation (approximately 0.003−0.004) was measured in each experiment, but has not been subtracted from the rates plotted here.

occurs only after a lag. As shown in Figure 3 (closed circles), higher concentrations of Ca^{2+} shorten the lag time, reaching a minimum at about 100 μM Ca^{2+}. Even at these concentrations, however, the lag is still perceptible, with 20−30 s being required after Ca^{2+} addition before lipid movement commences. This lag might correspond to the time required for internal Ca^{2+} levels to become elevated, with the longer lag times at low Ca^{2+} levels resulting from a slower rate of Ca^{2+} accumulation in the cells. To test this possibility, DO11.10 cells were loaded with Calcium Green-5N, a Ca^{2+}-sensitive fluorescent probe, and the half-time for maximal fluorescence increase was measured as a function of external Ca^{2+} levels. As shown in Figure 3, this time (open circles) is much shorter than the lag time for scramblase activation (closed circles) and is not sensitive to the levels of Ca^{2+} added over the range used to induce the scramblase. These results suggest that the lag does not reflect the time required for Ca^{2+} levels

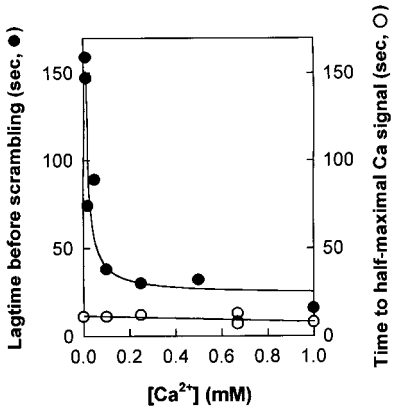

FIGURE 3: Lag time before scrambling as a function of the extracellular Ca^{2+} concentration. The closed symbols represent the lag time, which is defined as the time between the addition of Ca^{2+} and the onset of the scrambling process as described in the text. The open symbols represent the half time for increase in Calcium Green signal, reflecting the internal Ca^{2+} concentration.

inside the cell to rise but rather represents the time required for increased Ca^{2+} levels to affect some event which is required for initiation of scramblase activity.

To determine whether the properties of scramblase activity were similar in other lymphoid cells, Jurkat cells, a human T-lymphocyte line, and EBV-transformed human B lymphocytes were examined. In these two cell lines, rates of scrambling were too slow to be reliably measured by the dithionite assay used for the DO11.10 cells. Therefore, another assay for scramblase activity was devised based on the appearance of endogenous PS on the cell surface as measured by binding of the PS-specific protein annexin V (*25*). In this assay, the scramblase was activated by ionophore and Ca^{2+} in the presence of an excess of FITC-labeled annexin V; externalization of PS and consequent binding of labeled annexin V results in cell-associated fluorescence, which was measured by flow cytometry. In Figure 4 are the scramblase activation profiles generated by this assay for both Jurkat (upper curve) and EBV-transformed B (middle curve) lymphocytes. As was observed with the dithionite assay in DO11.10 cells, activation of the scramblase after addition of ionophore was preceded by a lag, even more extended than that observed in DO11.10 cells. It should be noted that annexin binding to cells already exposing PS begins immediately (data not shown), and the lag thus is not due to the time required for annexin binding. Moreover, the lags are observed at the high external Ca^{2+} levels (mM) required for efficient annexin V binding and are thus not due to insufficient Ca^{2+}.

Although the lag times are similar in these two cell types, the rate of PS externalization is different, being faster in the Jurkat cells than in the EBV-transformed B cells. These rates, in turn, are slower than those observed in DO11.10 cells using the continuous dithionite reduction assay. The annexin V binding assay could not be used to confirm the high rate of scrambling in DO11.10 cells because the assay is limited by the rate of annexin binding, which was slower than the rate of scrambling in these cells. To circumvent this limitation, we made use of a dye molecule, FM1−43, whose binding was recently reported to be sensitive to scramblase activation (*24*). We confirmed that addition of this probe resulted in about 10-fold higher levels of fluorescence from

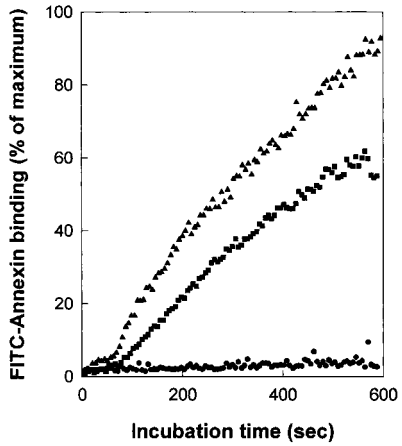

FIGURE 4: Time course of FITC-labeled annexin V binding to ionophore treated lymphoid cells. Jurkat cells (triangles), EBV-transformed B cells from a normal subject (squares) and EBV-transformed B cells from a patient with Scott syndrome (circles) were preincubated with FITC-annexin for 5 min in annexin binding buffer. Ionomycin was then added, and the incubation mixture immediately transferred to a flow cytometer. Fluorescence intensity of the morphologically normal, PI-negative cell population was monitored for 10 min, and expressed as a fraction of the maximal binding obtained with apoptotic cells after incubation for 15 min. Details are given in Materials and Methods.

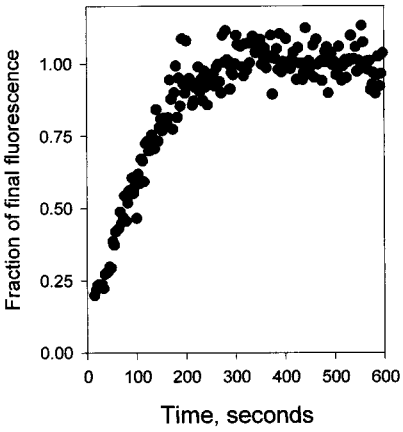

FIGURE 5: Time course of FM1−43 binding to ionophore treated DO11.10 lymphoid cells. FM1−43 was added to a final concentration of 3 μM to DO11.10 cells suspended in annexin binding buffer as in Figure 4. Ionomycin was then added, and the incubation mixture immediately transferred to a flow cytometer. Fluorescence intensity of the morphologically normal cells was monitored and plotted as fraction of the final plateau value.

apoptotic or ionophore stimulated cells than from viable or unstimulated cells; the difference in fluorescence was similar in EBV-transformed B cells, Jurkats, and DO11.10 cells (data not shown). We therefore investigated whether this probe could be substituted for annexin V in the continuous cytometer assay, and found that annexin V and FM1−43 gave similar results when applied to ionophore stimulated EBV-transformed B cells (data not shown), except that binding of the dye to the apoptotic cell fraction (where lipid asymmetry was already abolished) was too rapid to measure. We therefore used the increase in FM1−43 fluorescence to confirm the rate of scramblase-induced lipid rearrangements in DO11.10 cells. As shown in Figure 5, using this assay, ionophore addition to DO11.10 cells was observed to give a rapid change in probe binding following an initial lag, as was observed with the NBD-PS probes and dithionite

Table 1: Phospholipid Scramblase Rates

cells	background lipid movement (sec^{-1}) × 10^3	scramblase-catalyzed movement (sec^{-1}) × 10^3
erythrocytes (human)[a]	0.015	0.45
platelets (human)[b]	1.8	78
DO11.10 (mouse)[c]	3.6	24
DO11.10 (mouse)[d]		13
jurkat (human)[e]		3.3
jurkat (human)[f]	0.27	5.6
EBV-transformed B (human)[e]		1.6
EBV-transformed B (human)[g]	0.11	1.0

[a] Calculated from data in ref *8*. [b] Calculated from data in ref *22*. [c] Calculated from the continuous assay using dithionite reduction of NBD-lipid analogues (Figure 1 of the present study). [d] Calculated from the continuous cytometric analysis using FM1-43 (Figure 5 of present study). [e] Calculated from the exposure rate of endogenous PS measured by FITC-labeled annexin V (Figure 4 of the present study). [f] Calculated from the uptake of NBD-PS in ionophore-treated cells (data not shown). [g] Calculated from the uptake of NBD-PS in ionophore-treated cells (Figure 6 of present study).

quenching. Together, these data confirm that the scramblase in DO11.10 cells mediates a high rate of lipid movement when activated. A summary of scramblase rates in these various lymphoid cells, and in human erythrocytes and platelets, is shown in Table 1. These results indicate that while scramblase rates vary by more than an order of magnitude between different lymphoid cells, the rates occupy a middle ground between the very fast scramblase rates in human platelets and the much slower scramblase rates in human erythrocytes.

The scramblase in platelets and erythrocytes is a catalyst of bidirectional transbilayer movement of all classes of membrane phospholipids (*8*, *22*, *26*). The assays used above demonstrate only that elevation of cytoplasmic Ca^{2+} enhances the rate of PS movement from inner to outer membrane leaflet of lymphoid cells. To determine the simultaneous effect on inward movement of PS in these cells, and to establish the effects on other phospholipids, measurements were made of the rates of internalization of NBD-labeled lipids introduced into the external leaflet, using extraction with BSA (*8*) to remove label remaining on the external side of the membrane before analysis by flow cytometry. As shown in Figure 6, internalization of NBD-phospholipids by untreated EBV-transformed B cells is strongly headgroup-dependent: NBD-PS is rapidly internalized, while NBD-PC mainly remains in the external leaflet, behavior characteristic of the aminophospholipid translocase that maintains lipid asymmetry in normal cells. However, following treatment with ionophore and Ca^{2+}, both NBD-PS and NBD-PC become internalized at the same rate and to the same extent (Figure 6, closed symbols); the rates measured with this assay are comparable to those measured by annexin binding in Figure 4, indicating that the annexin itself neither promoted nor retarded scramblase activity. These results demonstrate that the transbilayer lipid movement catalyzed by elevated Ca^{2+} levels in lymphocytes is bidirectional and not specific to the polar headgroup of the lipid; these are the same characteristics that define the scramblase in platelets and erythrocytes.

In patients with Scott syndrome, a rare bleeding disorder (*14*), ionophore and Ca^{2+} do not activate the scramblase in either platelets or erythrocytes (*11*, *13*). To confirm the relationship of the scramblase in lymphoid cells with that in platelets and erythrocytes, EBV-transformed B cells from a patient with Scott syndrome were examined for exposure of PS following Ca^{2+} and ionophore treatment. As shown in Figure 4 (lower curve), no detectable exposure of endogenous PS occurs in these cells over a period of 10 min following ionophore addition, a time sufficient for PS exposure in control EBV-transformed cells to be almost half completed (middle curve). Measurements of NBD-PS internalization after addition of ionophore to Scott cells indicated that rapid movement of this probe had ceased (data not shown), indicating that the translocase was inactivated by this treatment as usual.

In addition to its role in exposing PS during platelet activation, the scramblase is also active in the exposure of

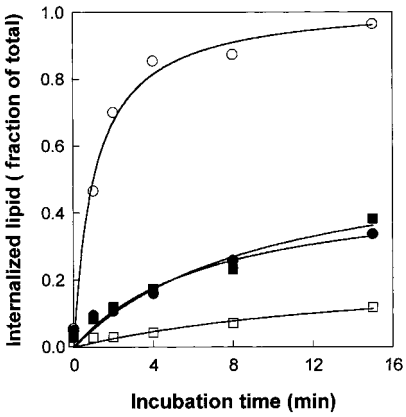

FIGURE 6: Uptake of NBD-lipid analogues in morphologically normal EBV-transformed B cells. Cells were incubated with NBD-PS (circles) or NBD-PC (squares) and samples were diluted in buffer with and without BSA and analyzed by flow cytometry as explained in Materials and Methods. PI-negative cells with normal light scatter were gated (see inset, Figure 9A) and their fluorescence intensities recorded. Percent internalized lipid was obtained by dividing fluorescence of samples with BSA by fluorescence of samples without BSA, and plotted vs time. Open symbols represent untreated cells, and closed symbols represent cells pretreated for 5 min with ionophore-Ca^{2+}.

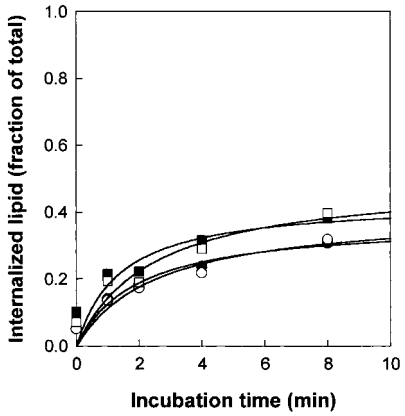

FIGURE 7: Effect of ionomycin on NBD-lipid uptake in apoptotic B cells. A culture of B cells containing approximately 22% morphologically apoptotic cells was treated with ionomycin (5 mM) in the presence of Ca^{2+} (1 mM) for 5 min. Subsequently, NBD-PS (circles) or NBD-PC (squares) was added, and samples taken at various times thereafter were diluted in buffer with or without BSA and percent probe internalized determined, as for Figure 5, for PI-negative apoptotic cells in the absence (open symbols) or presence (closed symbols) of ionophore.

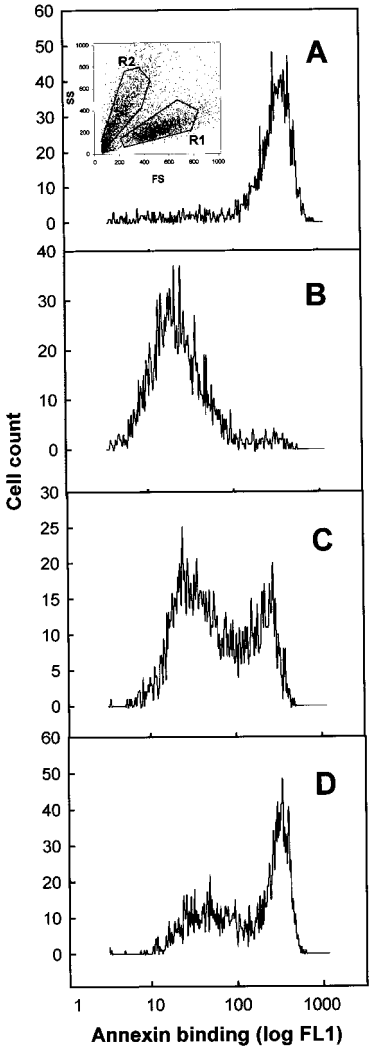

FIGURE 8: Binding of FITC-labeled annexin V to EBV-transformed Scott B cells after exposure to UV-radiation. (A) Histogram of the binding of annexin V to spontaneously apoptotic cells with abnormal light scatter (R2). Insert: light scatter profile used to gate cells with a normal profile (R1) and apoptotic cells with an abnormal profile (R2). (B−D) Binding of annexin V to cells in the R1 population at 0 (B), 180 min (C) and 240 min (D) after UV irradiation.

PS during apoptosis (*17*, *19*, *20*), an important physiological process in lymphoid cells. To ask whether the scramblase activated in apoptotic cells is the same as the scramblase activated artificially by Ca^{2+}, the characteristics of the scramblase in apoptotic cells were examined. Because activation of the scramblase among apoptotic cells in a population is asynchronous over several hours, continuous assays of PS exposure are not appropriate for analysis of the apoptotic scramblase activation. However, scrambling activity can be analyzed by applying the NBD-phospholipid internalization assay to frankly apoptotic cells, gated for separate analysis on the basis of their altered light scattering in FS/SS plots (see Figure 8, below). Uptake of these probes in apoptotic B cells (Figure 7, open symbols) closely resembled the uptake seen in cells with normal morphology following ionophore treatment (Figure 6, closed symbols). Similar results were observed with Jurkat cells (data not shown). The similar lack of specificity for headgroup, combined with the bidirectionality implied by these data and the annexin binding results, suggests that the properties of

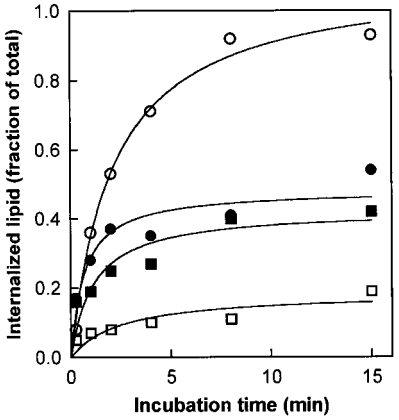

FIGURE 9: Uptake of NBD-lipid analogues in EBV-transformed Scott cells. NBD-PS (circles) or NBD-PC (squares) were added to a culture of Scott B cells containing approx 70% cells with normal light scatter and 30% apoptotic cells with abnormal light scatter. Samples taken at various times were diluted in buffer with or without BSA and percent probe internalized determined, as for Figure 5, for PI-negative cells with normal light scatter (open symbols) and apoptotic cells with abnormal light scatter (closed symbols).

the scramblase activated in apoptotic cells resemble those of the scramblase activated by ionophore and Ca^{2+}. In addition, these measurements imply that the rates of lipid movement that result are similar and independent of mechanism by which the scramblase is activated. If the scramblase which is activated in these two cases is the same, then addition of ionophore to apoptotic cells should not increase scramblase activity. As shown in Figure 7, ionophore and Ca^{2+} did not increase the rate of NBD-PC or -PS internalization in apoptotic cells, arguing that the scramblase activities induced by these two conditions are one and the same.

As indicated above, the scramblase is not activated in Scott cells treated with Ca^{2+} and ionophore. If the Ca^{2+} and apoptotic activation of the scramblases use identical mechanisms, apoptotic Scott cells would not be expected to expose PS. However, as shown in Figure 8A, spontaneously apoptotic Scott cells bind annexin V, indicating that PS is exposed on their surface. Moreover, upon induction of apoptosis by exposure to UV, the increase in the frequency of apoptosis results in the appearance of a significant number of annexin V positive cells in the morphologically normal, as well as in the morphologically apoptotic, population of Scott cells (Figure 8, panels B−D). The annexin V positive cells appear at about the same time as found for normal EBV-transformed B cells which were analyzed in parallel (data not shown). The appearance of annexin V positive cells in the morphologically normal population of both control (data not shown) and Scott cells indicates that in both cell types, exposure of PS precedes the cell shrinkage and loss of membrane integrity that occur during apoptosis. To examine the characteristics of lipid movement in spontaneously apoptotic Scott cells, NBD-PS and NBD-PC internalization were compared in morphologically normal and morphologically apoptotic Scott cells. As shown in Figure 9, apoptotic Scott cells show the reduction in NBD-PS internalization expected from translocase inactivation. However, as in normal cells when scramblase is activated by either Ca^{2+} or apoptosis, a substantial residual rate of internalization of PS is observed, comparable to the increased NBD-PC internalization rate. Together these data strongly suggest that the scramblase is

fully activated in apoptotic Scott cells, and thus that activation by this pathway is not affected by the Scott defect.

DISCUSSION

Scramblase has been most extensively characterized in platelets and erythrocytes, two specialized cell types which might be expected to represent extremes of the functional spectrum. In platelets, rapid and efficient exposure of PS is essential to the platelet's role in catalyzing thrombin formation (*27*), and the scramblase in these cells is correspondingly highly active (*22*). Erythrocytes, on the other hand, must circulate for long times and in high numbers without catalyzing coagulation, and mammals may even depend on the suppression of PS exposure for their formation at the stage of enucleation (*1*); the scramblase activity in these cells can be quite low, or even absent in cases such as porcine erythrocytes (*28*). In the lymphoid cells examined here, scramblase rates fall between these two extremes. Remarkably, though, there is a lag before onset of lipid movement when scrambling is initiated by raising intracellular Ca^{2+} levels. In continuous assays with platelets, a brief pause before elevated lipid movement begins is sometimes observed, but such pauses are only a few seconds long; the lag of 30 s or more seen in these lymphoid cells is much longer (and generally longer than the entire time course of NBD-PS externalization in platelets). In erythroid cells, on the other hand, the scramblase is so slow, and the assays used to measure it of correspondingly low resolution, that the presence of such a lag phase may well have gone unnoticed. The lag may thus be present in these two cases, but if so must be of much shorter duration in platelets, without being proportionately extended in erythrocytes. In any event, the existence of this lag following the much faster rise in cytoplasmic Ca^{2+} suggests that there are one or more intervening steps between the elevation of Ca^{2+} levels and activation of the lipid scrambling process itself. These results call attention to the existence and potential importance of the Ca^{2+}-dependent activation process, as quite distinct from the activity which actually catalyzes transbilayer lipid movement. The similarity in characteristics of the scrambling process—bidirectionality and nonspecificity with respect to lipid polar headgroup—suggests that the same type of scramblase is activated by Ca^{2+} in lymphoid cells, platelets and erythrocytes. Differences in rates of lipid movement between these cells may reflect differences in number of copies of the scramblase protein itself present in the plasma membranes of these cells.

An important issue is the relation between the scramblase activities induced by Ca^{2+} and by apoptosis. The presence of the scramblase activity in apoptotic cells can be inferred from the exposure of PS and the elevation of PC internalization. These bidirectional and nonspecific characteristics of apoptotic activity mirror those of Ca^{2+}-induced activity. The detailed characteristics of the apoptotic scramblase activity are difficult to investigate, because the induction of apoptosis occurs over a much longer time scale (hours) than the entire scrambling process (minutes). Nevertheless, in two of the cells used here (Jurkat and EBV-transformed B cells), apoptotic cells with intact plasma membranes can be identified by flow cytometry on the basis of their light scatter characteristics, combined with impermeability to propidium iodide, and the uptake of NBD-lipid probes by these cells can thus be examined directly. These cells display the nonspecific bidirectional phospholipid movement that was observed in previous studies on activated platelets and Ca^{2+}-treated erythrocytes (*22*, *26*). This raises the question of whether the enhanced transbilayer movement observed during apoptosis and that induced by Ca^{2+} is mediated by a single type of scramblase activated through different pathways or alternatively, that more than one scramblase is operative. A number of observations argue in favor of the first option: (i) in both Ca^{2+}- or apoptosis-induced scrambling, the rate of transbilayer lipid movement is insensitive to lipid headgroup, and bidirectional (at least for PS); (ii) once the scrambling process is activated in apoptotic cells, the rates of lipid movement across the bilayer are very similar to those in Ca^{2+}-activated cells; (iii) no increase in rate of lipid scrambling is seen when both pathways are activated, i.e., when apoptotic cells are treated with ionophore. The fact that apoptotic Scott B cells exhibit a scrambling process which is not different from that of apoptotic normal B cells was somewhat surprising. If the apoptosis- and Ca^{2+}-induced scramblase are not different, this result would suggest that lymphoid cell scramblase can be activated by different pathways. This possibility is compatible with the observation that lipid scrambling induced by Ca^{2+} is completely absent in Scott platelets, but the rate and extent of scrambling induced by the combined action of collagen and thrombin amounts to ~30% of those in normal controls (*26*). In this respect it is worthwhile to mention that Zhou and co-workers (*29*) found normal levels of expression of mRNA and protein of a candidate scramblase in Scott lymphoblasts. On the basis of these and other findings, these authors concluded that scramblase in Scott cells is identical to that in normal cells and that the defect in Scott cells may be related to aberrant processing or regulation of the scramblase.

The possibility that a single scramblase is activated by different pathways in apoptosis and during platelet activation suggests that these two processes could be independently regulated and could be made independent targets of pharmacological intervention. The alternative possibility is that there are different scramblases (with different activation pathways) in these two cell types; this possibility cannot be ruled out until the scramblase and the steps which lead to its activation are unambiguously characterized at the molecular level.

ACKNOWLEDGMENT

We thank the Edmond Hustinx Foundation, Maastricht, The Netherlands, for their support of a visiting professorship for P.W. at the Cardiovascular Research Institute Maastricht.

REFERENCES

1. Williamson, P., and Schlegel, R. A. (1994) *Mol. Membr. Biol. 11*, 199−216.
2. Zwaal, R. F. A., and Schroit, A. J. (1997) *Blood 89*, 1121−1132.
3. Van den Eijnde, S. M., Boshart, L., Reutelingsperger, C. P. M., DeZeeuw, C. I., and Vermeij-Keers, C. (1997) *Cell Death Differ. 4*, 311−316.
4. Seigneuret, M., and Devaux, P. F. (1984) *Proc. Natl. Acad. Sci. U.S.A. 81*, 3751−3755.
5. Tang, X., Halleck, M. S., Schlegel, R. A., and Williamson, P. (1996) *Science 272*, 1495−1497.

6. Zwaal, R. F. A., Comfurius, P., and Bevers, E. M. (1998) *Biochim. Biophys. Acta 1376*, 433−453.
7. Fadok, V. A., Voelker, D. R., Campbell, P. A., Cohen, J. J., Bratton, D. L., and Henson, P. M. (1992) *J. Immunol. 148*, 2207−2216.
8. Williamson, P., Kulick, A., Zachowski, A., Schlegel, R. A., and Devaux, P. F. (1992) *Biochemistry 31*, 6355−6360.
9. Zwaal, R. F. A., Comfurius, P., and Bevers, E. M. (1993) *Biochem. Soc. Trans. 21*, 248−253.
10. Williamson, P., Bevers, E. M., Smeets, E. F., Comfurius, P., Schlegel, R. A., and Zwaal, R. F. A. (1995) *Biochemistry 34*, 10448−10455.
11. Bevers, E. M., Wiedmer, T., Comfurius, P., Shattil, S. J., Weiss, H. J., Zwaal, R. F. A., and Sims, P. J. (1992) *Blood 79*, 380−388.
12. Zhou, Q. S., Zhao, J., Stout, J. G., Luhm, R. A., Wiedmer, T., and Sims, P. J. (1997) *J. Biol. Chem. 272*, 18240−18244.
13. Toti, F., Satta, N., Fressinaud, E., Meyer, D., and Freyssinet, J. M. (1996) *Blood 87*, 1409−1415.
14. Weiss, H. J. (1994) *Sem. Hematol. 31*, 312−319.
15. Pradhan, D., Krahling, S., Williamson, P., and Schlegel, R. A. (1997) *Mol. Biol. Cell 8*, 767−778.
16. Krahling, S., Callahan, M. K., Williamson, P., and Schlegel, R. A. (1999) *Cell Death Differ. 6*, 183−189.
17. Verhoven, B., Krahling, S., Schlegel, R. A., and Williamson, P. (1999) *Cell Death Differ. 6*, 262−270.
18. Callahan, M. K., Williamson, P., and Schlegel, R. A. (2000) *Cell Death Differ. 7*, 645−653.
19. Verhoven, B., Schlegel, R. A., and Williamson, P. (1995) *J. Exp. Med. 182*, 1597−1601.
20. Bratton, D. L., Fadok, V. A., Richter, D. A., Kailey, J. M., Guthrie, L. A., and Henson, P. M. (1997) *J. Biol. Chem. 272*, 26159−26165.
21. Bevers, E. M., Tilly, R. H., Senden, J. M., Comfurius, P., and Zwaal, R. F. A. (1989) *Biochemistry 28*, 2382−2387.
22. Williamson, P., Bevers, E. M., Smeets, E. F., Comfurius, P., Schlegel, R. A., and Zwaal, R. F. A. (1995) *Biochemistry 34*, 10448−10455.
23. Mcintyre, J. C., and Sleight, R. G. (1991) *Biochemistry 30*, 11819−11827.
24. Zweifach, A. (2000) *Biochem. J. 349*, 255−260.
25. Koopman, G., Reutelingsperger, C. P. M., Kuijten, G. A. M., Keehnen, R. M. J., Pals, S. T., and van Oers, M. H. J. (1994) *Blood 84*, 1415−1420.
26. Smeets, E. F., Comfurius, P., Bevers, E. M., and Zwaal, R. F. A. (1994) *Biochim. Biophys. Acta 1195*, 281−286.
27. Rosing, J., Bevers, E. M., Comfurius, P., Hemker, H. C., van Dieijen, G., Weiss, H. J., and Zwaal, R. F. A. (1985) *Blood 65*, 1557−1561.
28. Bevers, E. M., Wiedmer, T., Comfurius, P., Zhao, J., Smeets, E. F., Schlegel, R. A., Schroit, A. J., Weiss, H. J., Williamson, P., Zwaal, R. F. A., and Sims, P. J. (1995) *Blood 86*, 1983−1991.
29. Zhou, Q. S., Sims, P. J., and Wiedmer, T. (1998) *Blood 92*, 1707−1712.

BI001929Z